# Study of the $^{50}$V Nucleus with the ($^3$He, $d$), ($^3$He, $\alpha$), ($^3$He, $p$), and ($^3$He, $p\gamma$) Reactions*

J. W. Smith†
*Argonne National Laboratory, Argonne, Illinois 60439, and Indiana University, Bloomington, Indiana 47401*

L. Meyer-Schützmeister and T. H. Braid
*Argonne National Laboratory, Argonne, Illinois 60439*

P. P. Singh
*Indiana University, Bloomington, Indiana 47401*

and

G. Hardie
*Western Michigan University, Kalamazoo, Michigan 49001*
(Received 29 June 1972)

The nucleus $^{50}$V has been studied with the $^{49}$Ti($^3$He, $d$), $^{51}$V($^3$He, $\alpha$), $^{48}$Ti($^3$He, $p$), and $^{48}$Ti($^3$He, $p\gamma$) reactions induced by the $^3$He$^{++}$ beam from the Argonne tandem Van de Graaff. The ($^3$He, $d$), ($^3$He, $\alpha$), and ($^3$He, $p$) angular distributions at $E(^3\text{He}) = 22$ MeV and with 20-, 30-, and 75-keV over-all resolution, respectively, have been analyzed with the distorted-wave Born approximation. The ($^3$He, $p$) and ($^3$He, $p\gamma$) reactions were also studied at 13 MeV to obtain the $\gamma$ decay of $^{50}$V levels (including two $0^+$ isobaric analog states) in which the neutron-proton pair is transferred with zero orbital angular momentum. The two $0^+$ isobaric analog states are observed to decay by $M1$ transitions to two different low-lying $1^+$ states, one of which is $f_{7/2}$ and the other is a complex configuration. Several levels between 1.3- and 4-MeV excitation energy are seen to decay in part to the $1^+$ levels populated by decay of the two $0^+$ analog states. The $^{50}$V levels at 1.333 and 1.490 MeV are assigned $1^+$, and the previous tentative spin assignments $5^+$, $4^+$, $3^+$, and $2^+$ of the first four excited states are supported. All available data are used to evaluate two models: (1) the truncated $1f_{7/2}$ shell model of McCullen, Bayman, and Zamick and (2) the Coriolos-coupling model of Wasielewski and Malik.

## I. INTRODUCTION

The odd-odd nucleus $^{50}$V may be described rather simply in the shell model as $(\pi f_{7/2})^3(\nu f_{7/2})^{-1}$ plus a $^{48}$Ca core. Two types of shell-model calculations may be readily applied to $^{50}$V. First, the McCullen, Bayman, and Zamick[1] (MBZ) truncated shell model, which considers only $1f_{7/2}$ active nucleons, predicts energy levels and wave functions for the states of $^{50}$V. These wave functions are used to calculate spectroscopic factors of one-nucleon-transfer reactions. Second, the Coriolis-coupling model of Wasielewski and Malik[2] may be used to calculate $^{50}$V energy levels and wave functions. The results of calculations with both approaches will be compared with experimental results.

Until recently, the $^{50}$V nucleus had been studied by only a few authors.[3-7] In the present work, the $^{49}$Ti($^3$He, $d$)$^{50}$V and $^{51}$V($^3$He, $\alpha$)$^{50}$V reactions were studied by measuring the angular distributions and extracting the orbital angular momentum transfers and spectroscopic factors. Further, the $^{48}$Ti($^3$He, $p$)-$^{50}$V two-nucleon-transfer reaction was measured, since it was expected to lead to two $0^+$ analog states whose nuclear configurations are approximately known from the study of their parent states.[8,9] Finally, the $\gamma$ decay of the levels populated by the ($^3$He, $p$) reaction with orbital angular momentum $L_{np} = 0$ was studied with the ($^3$He, $p\gamma$) reaction. In particular, the $\gamma$ decays of the two analog states of known configuration were observed, and the wave functions of the states so populated are inferred.

## II. EXPERIMENTAL PROCEDURE

### A. $\gamma$-Decay Measurement

A 13-MeV $^3$He beam from the Argonne tandem Van de Graaff was incident on a 1-mg/cm$^2$ metallic $^{48}$Ti foil and was stopped by a 0.003-in. gold foil placed immediately behind it. The highly energetic protons from the ($^3$He, $p$) reaction on $^{48}$Ti passed through the gold foil and were energy analyzed in a pair of totally depleted silicon surface-barrier detectors in tandem. These detec-

tors subtended an angular range of ±10° with respect to the beam. A Ge(Li) $\gamma$ detector was positioned at 80° to the incident beam.

Pairs of linear signals from the detectors were tested for time coincidence (within 80 nsec) and for freedom from distortion (e.g., from pileup). If the pair of linear signals was found acceptable, it was analyzed as a two-parameter event in a $10^6$- channel pulse-height analyzer which has been described in detail elsewhere.[10]

The particle spectrum with no coincidence requirement is shown in Fig. 1(a). The poor resolution [300 keV full width at half maximum (FWHM)] results from the energy loss of $^3$He ions in the 1-mg/cm$^2$ target and the proton or deuteron energy straggling in the gold foil. The peaks between channels 400 and 750 are due to the ($^3$He, $p$) reaction, while peaks below channel 400 result from the ($^3$He, $d$) reaction. The ($^3$He, $d\gamma$) measurement was simultaneous with the ($^3$He, $p\gamma$) measurement. Figure 1(b) presents the particle spectrum in coincidence with any $\gamma$ ray. The knocked-on protons from the $^1$H($^3$He, $p$)$^3$He reaction [at channel 280 in Fig. 1(a)] are eliminated in Fig. 1(b) because no $\gamma$ ray is associated with them and the accidental coincidence rate is low.

Figure 2 is the $\gamma$ spectrum in coincidence with protons from the reaction populating the $^{50}$V analog state at 4.816 MeV, which is seen to decay by 3483- and 947-keV $\gamma$ rays in cascade. The other $\gamma$ rays arise from decays of nearby levels that overlap the 4.816-MeV excitation peak in the proton spectrum. The $\gamma$-ray energies were determined to within ±10 keV (except that the 7098-keV $\gamma$ ray is uncertain to ±25 keV) and the energy levels seen in the $\gamma$ decay are assigned an uncertainty of ±15 keV.

The $\gamma$ decay scheme is presented in Fig. 3. 11 of the $^{50}$V levels (shown as solid lines) have been populated strongly enough to allow the determina-

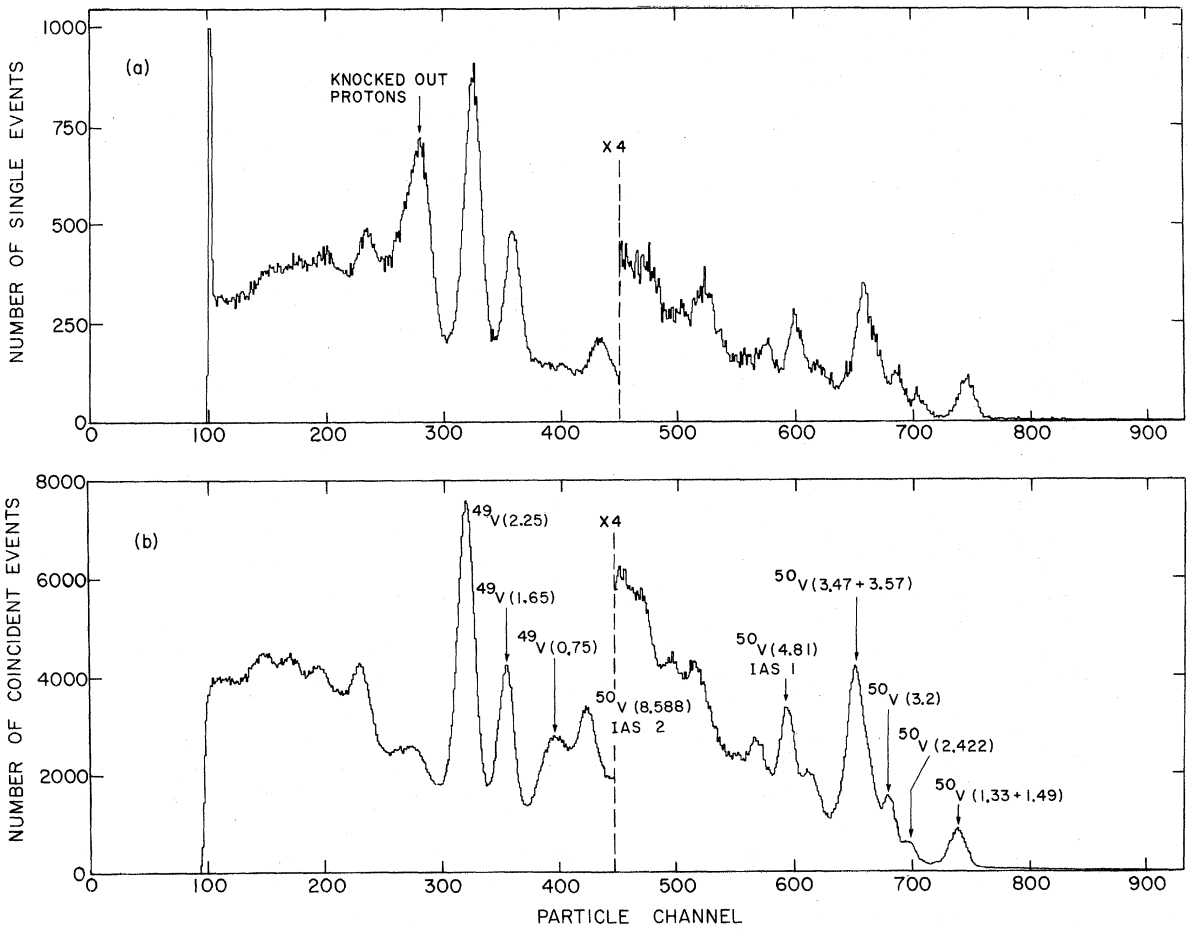


FIG. 1. Particle spectra from 13-MeV $^3$He$^{++}$ on $^{48}$Ti. The detector was at 0°. (a) Spectrum with no coincidence requirement. (b) Spectrum of particles coincident with $\gamma$ rays (within 80 nsec).

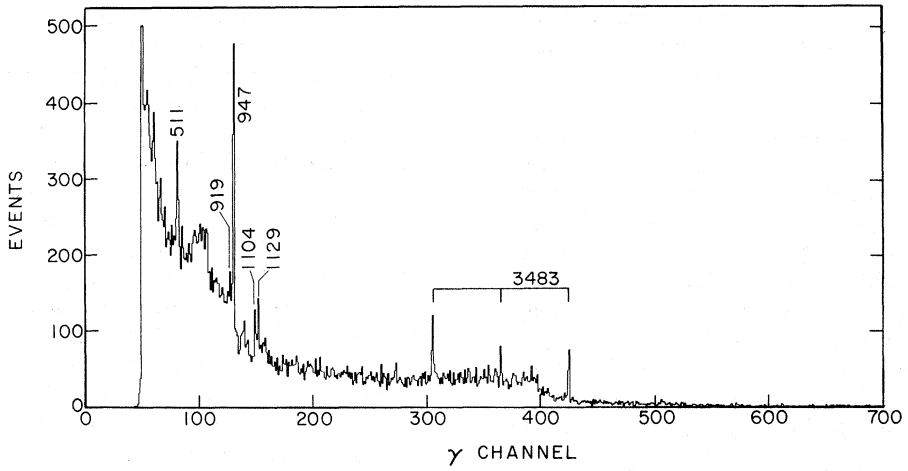


FIG. 2. The spectrum of $\gamma$ rays in coincidence with protons from the $^{50}$V isobaric analog state at 4.816 MeV. The bracket connects the full-energy, single-escape, and double-escape peaks of the 3483-keV $\gamma$ ray.

tion of their $\gamma$ decay. In addition, three levels (dashed lines) are populated by the primary $\gamma$ decay of higher levels, and the $\gamma$ decays of two of these are determined. The $\gamma$-ray cascade from the third level[4] at 0.386 MeV is not observed because all the $\gamma$ rays in the cascade are below the low-energy $\gamma$ cutoff in this measurement.

Each of the two analog states decays preponderantly (>80%) by a single branch. Likewise, the levels at 1.333 and 1.490 MeV appear to have one-branch decays (<20% via other branches). In the decays of all other levels, a branch with an intensity as high as 40% of that of the strongest observed $\gamma$ ray from that level could be missed

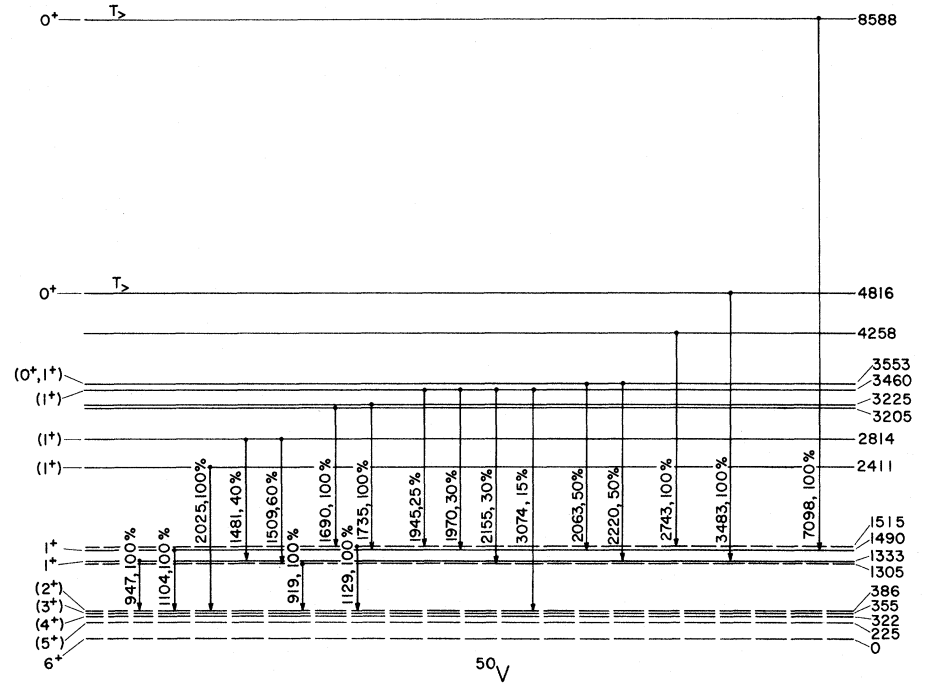


FIG. 3. The observed $\gamma$ decay of levels in $^{50}$V assuming isotropic distributions. Levels populated by the ($^3$He, $p$) reaction with $L_{np}=0$ or $L_{np}=0+2$ are shown as solid lines. Dashed lines are levels that participate in the cascades but are not populated directly by the ($^3$He, $p$) reaction.

either because of the small cross section with which the level is populated or because the $\gamma$ decay is divided among many branches.

### B. Charged-Particle Spectroscopy

The angular distributions of the ($^3$He, $d$), ($^3$He, $\alpha$), and ($^3$He, $p$) reactions have been studied with the Argonne split-pole magnetic spectrograph described elsewhere.[11] The good energy resolution of this instrument allows the separation of many closely spaced $^{50}$V levels.

The light reaction products from the $^{49}$Ti($^3$He, $d$)-$^{50}$V and the $^{48}$Ti($^3$He, $p$)$^{50}$V were detected in the focal plane of the spectrograph with Kodak 50-$\mu$m NTB photographic emulsions. Foils of acetate were placed immediately in front of the emulsions to stop the scattered $^3$He and products of other reactions and also to maximize the specific ionization of the deuteron and proton in the emulsion. The number of tracks within a narrow momentum range on the emulsion was counted by an automatic plate scanner.[12]

Typical results are shown in Fig. 4 for the ($^3$He, $d$) reaction and in Figs. 5 and 6 for the ($^3$He, $p$). The over-all resolution was 20 keV FWHM for the ($^3$He, $d$) reactions and 75 keV FWHM for the ($^3$He, $p$) reaction. The ($^3$He, $p$) reaction was remeasured at one angle (7°) with 42-keV FWHM resolution to check for closely spaced levels.

For the $^{51}$V($^3$He, $\alpha$)$^{50}$V reaction, it is necessary to prevent light reaction products from obscuring the $\alpha$ tracks on the emulsion. This is done by taking advantage of the greater specific ionization of the $\alpha$ particle. In Ilford $K$-1 plates, singly charged light reaction products of energy >7 MeV leave no ionization tracks. Unfortunately the Ilford $K$-1 emulsion produced an $\alpha$ track of too low a spot density to be counted with the automatic scanner, so these emulsions were scanned by human scanners. A typical spectrum is shown in Fig. 7. The over-all resolution is 30 keV FWHM.

The peaks associated with most levels somewhat overlapped those of nearby levels. The spectral decomposition therefore required fitting them with the shapes obtained from isolated peaks in the spectrum.[13]

In order to determine the absolute cross section, one needs to know the target thickness. Therefore, the elastic scattering of 8-MeV $^3$He$^{++}$ by the target was measured at 12, 17, and 22° to the beam. Since the variation of the cross section with scattering angle agrees with that calculated from Rutherford scattering, no interference from nuclear scattering was assumed and the Rutherford cross sections were used to determine the thickness of the targets. The uncertainty in the absolute cross section is set at 25%.

Two problems encountered in the $^{49}$Ti($^3$He, $d$)$^{50}$V measurement deserve mention. First, after ap-

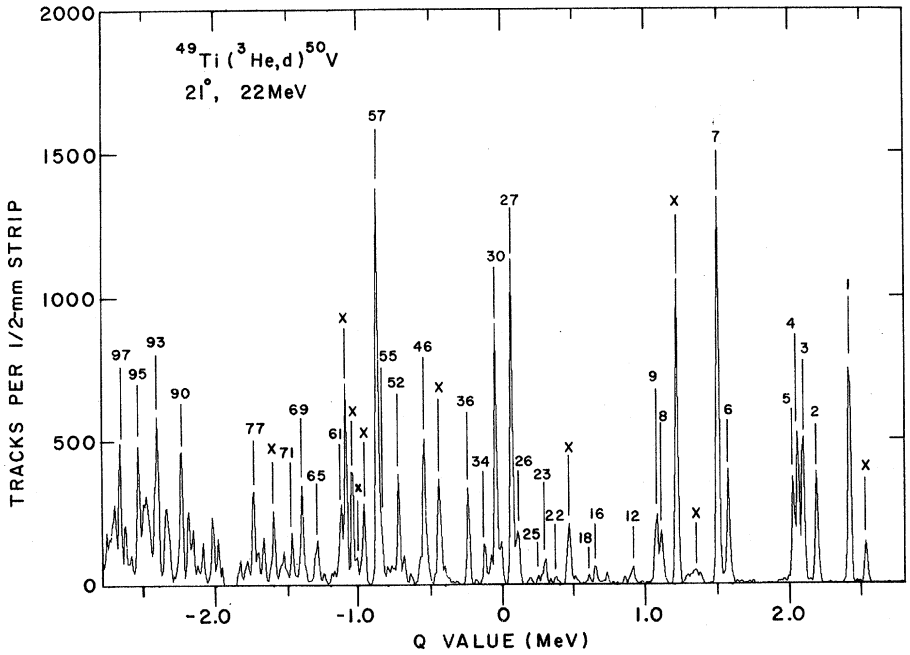


FIG. 4. A typical deuteron spectrum from the $^{49}$Ti($^3$He, $d$)$^{50}$V reaction induced by 22-MeV $^3$He. It was measured at 21° to the beam.

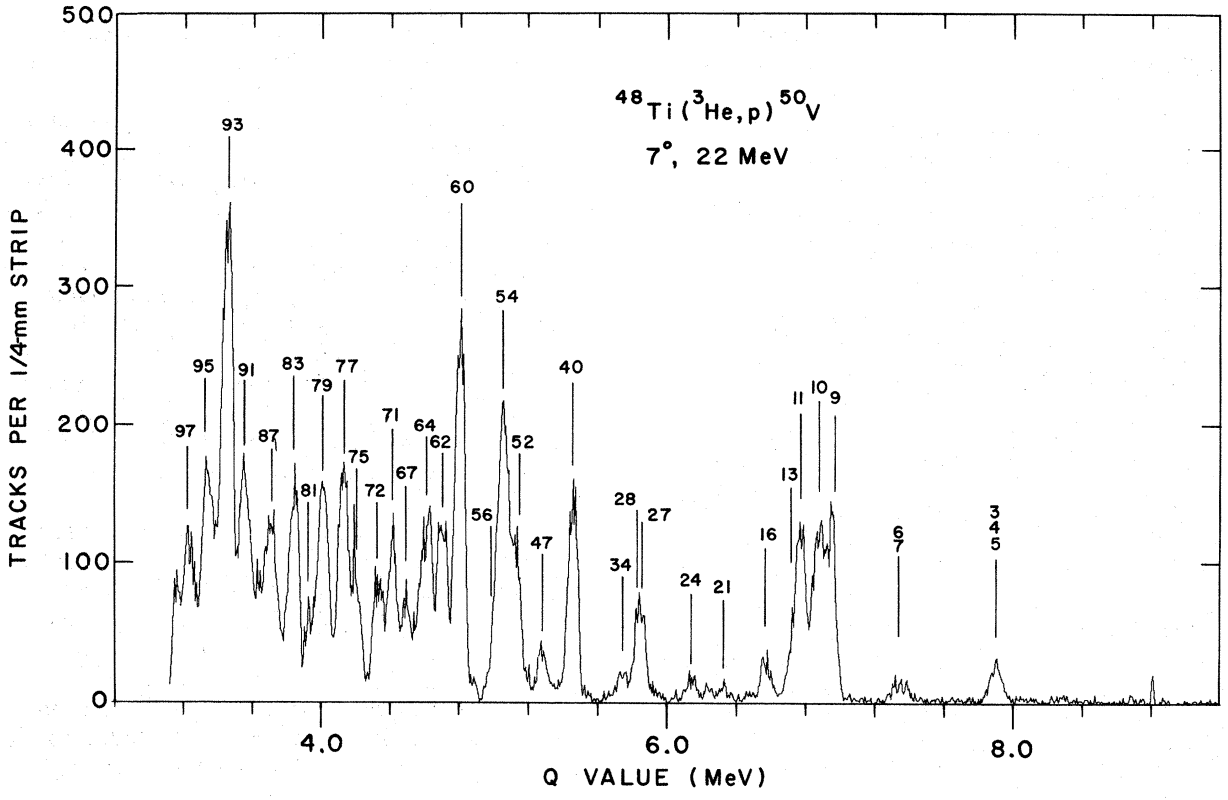


FIG. 5. A typical proton spectrum from the $^{48}$Ti($^3$He, $p$)$^{50}$V reaction induced by 22-MeV $^3$He particles. It was measured at 7° to the beam.

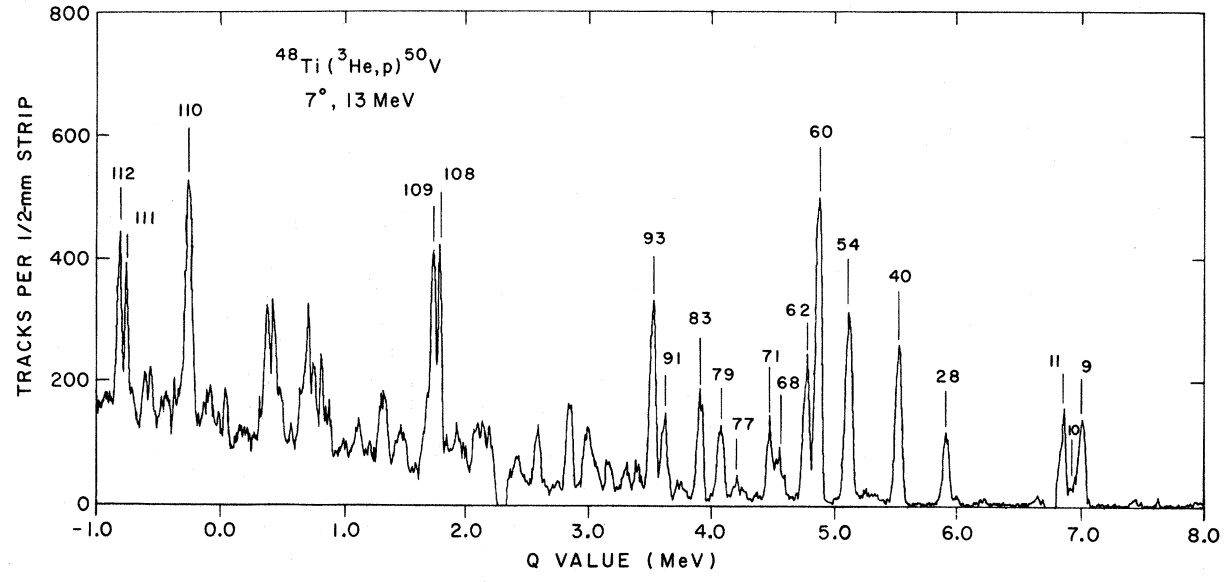


FIG. 6. A typical proton spectrum from the $^{48}$Ti($^3$He, $p$)$^{50}$V reaction induced by 13-MeV $^3$He. It was measured at 7° to the beam.

plying the distorted-wave Born approximation (DWBA) to correct for the energy difference between the recent measurements of Bishop *et al.*[3] at 15 MeV and the present study at 22 MeV, the absolute cross sections for this reaction disagree. At the first maximum of the ground-state angular distribution, the ratio of the cross section at 22 MeV (this work) to that at 15 MeV (Ref. 3) is 9:8, whereas the DWBA predicts ~2:1. If this discrepancy were due to phenomena which cannot be taken into account by the DWBA calculations, then comparisons between experimental data and DWBA calculations would not be meaningful. To check this possibility, we repeated the measurements to ensure that the 22- and 15-MeV data were obtained under identical conditions, and the ratio was then found to be 2.2:1 in agreement with the DWBA prediction. Hence, there is a discrepancy of about a factor of 2 between our measurements and those of Bishop *et al.*[3]

Second, although the $^{48}$Ti and $^{51}$V targets were better than 99% pure, the $^{49}$Ti target was enriched only to 76% in $^{49}$Ti, the major contaminants being $^{48}$Ti and $^{50}$Ti. In order to identify peaks from reactions on these contaminants, the $Q$ values of the observed peaks were inspected for a kinematic shift not consistent with target mass 49. Since the shift was to be 1 part in 50, 11 exposures were made from 7 to 90°. This was sufficient to identify peaks resulting from target mass 48 or 50; these peaks are marked × in Fig. 4.

## III. DWBA CALCULATIONS

The DWBA calculations were performed by use of the code DWUCK[14] with the parameters given in Table I. Good fits for the ($^3$He, $d$) and ($^3$He, $\alpha$) reactions were obtained with a finite-range parameter $R = 0.77$ fm and $R = 2$ fm, respectively. The results of the calculations are shown as smooth curves in Figs. 8 and 9, and the data are represented by points.

For the ($^3$He, $p$) reaction, the transferred neutron-proton pair was considered to be stripped off with a zero-range interaction. The measured points and representative calculated curves are shown in Figs. 10 and 11. The fits are generally much less successful than those for one-nucleon transfer but are sufficiently good to allow the extraction of the $L_{np}$ transfer.

For the $^{49}$Ti($^3$He, $d$)$^{50}$V reaction, the well defined shapes for different $l$ transfers (Fig. 8) have allowed the determination of $l$ values and the identification of transfers with mixed $l = 1$ and 3. The results of the analysis are presented in Table II, which gives the energies for all observed levels, the $l$ transfers, and the spectroscopic factors for the levels populated strongly enough to allow the determination. The $0^+$ analog state at 4.820 MeV

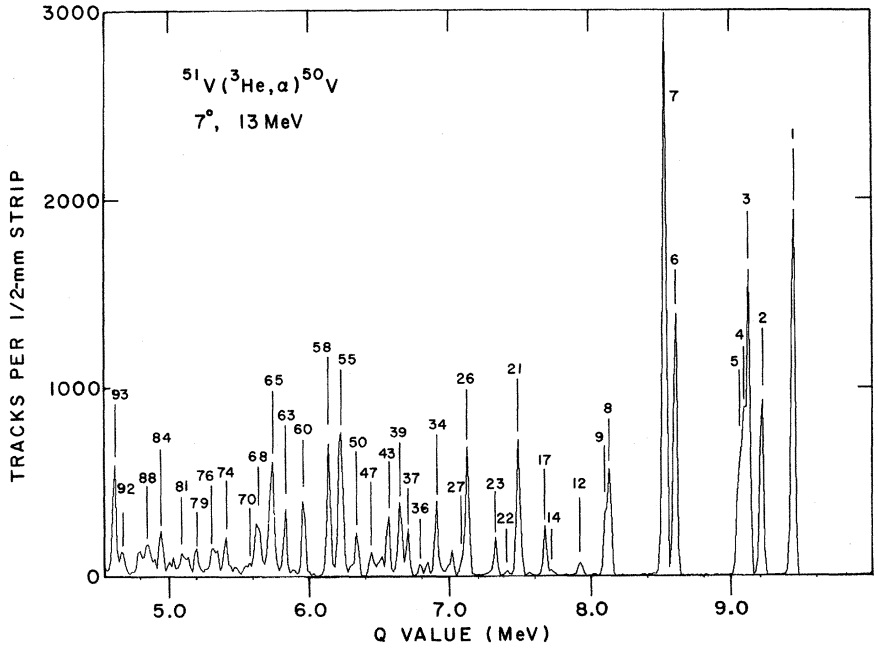


FIG. 7. A typical $\alpha$ spectrum from the $^{51}$V($^3$He,$\alpha$)$^{50}$V reaction induced at 22-MeV $^3$He. It was measured at 15° to the beam.

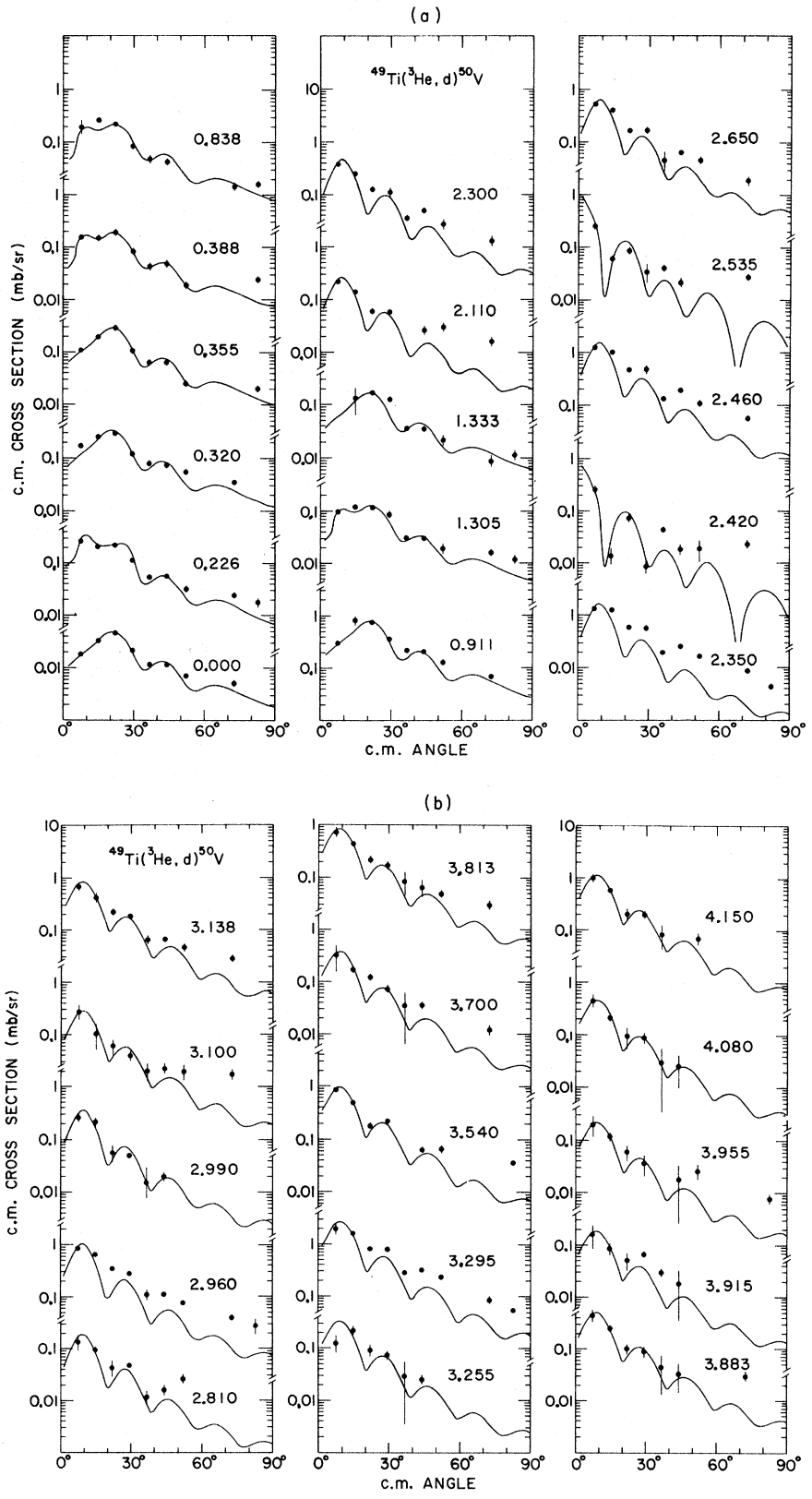


FIG. 8. Angular distributions and DWBA fits from the $^{49}$Ti($^3$He,$d$)$^{50}$V reaction induced by 22-MeV $^3$He.

is strongly populated, but nearby peaks prevent the determination of the angular distribution with any accuracy. In Fig. 12, the spectroscopic factors, plotted on a logarithmic scale, are presented as a function of excitation energy for $l=3$, 1, and 0.

The quasiexponential falloff of the ($^3$He, $\alpha$) angular distribution (Fig. 9) prevents the determination of admixtures of transferred orbital angular momentum. The states populated below 2 MeV are well fitted with $l=3$ neutron transfer, but the shapes of six levels (at 2.737, 2.790, 2.875, 2.930, 3.095, and 3.219 MeV) are sufficiently dissimilar to require a different value of $l$ for the transferred neutron. These six levels are fitted with $l=2$ or 0. The results of the ($^3$He, $\alpha$) reaction are tabulated in Table II, which also lists the ($d, p$) results.[6] The spectroscopic factors for $l=3$, 2, and 0 are plotted on a logarithmic scale in Fig. 13.

In general the results of the different particle reactions agree well, but a discrepancy exists for the level at 1.330 MeV excitation. Our work (Sec. V) requires a spin assignment of $1^+$ for this level, whereas the $^{49}$Ti($^3$He, $d$)$^{50}$V work of Bishop, Pullen, and Rosner[3] and the $^{51}$V($d, t$)$^{50}$V work of Sourkes, Ohnuma, and Hintz[6] show an angular momentum transfer $l=1+3$, which requires a spin assignment of $2^+-5^+$. In the work of Bishop, Pullen, and Rosner we attribute this discrepant result to the 155-keV level of $^{49}$V formed from a $^{48}$Ti contaminant in their target. This contaminant level, which would be within 20 keV of the peak of interest up to 45°, shows an $l=1$ transfer when populated by the ($^3$He, $d$) reaction.[15] The reason for the $l=1$ admixture in the neutron-pickup reaction of Sourkes, Ohnuma, and Hintz is less clear. The $l=1$ spectroscopic factor is very small, and we will assume that it is not a real admixture but appears due to ordinary statistical uncertainties in the data.[16]

The shapes of the ($^3$He, $p$) angular distributions (Figs. 10 and 11) are characteristic of $L_{np}$ transfer. Because the DWBA fits for deuteron transfer are much less satisfactory than those for one-nucleon transfer, measured angular distributions of similar shape are plotted together and a corresponding DWBA angular distribution (calculated for a $Q$ value in the middle of the range) is plotted above them. Table II lists the observed energy levels and the $L_{np}$ transfer assignments for the ($^3$He, $p$) reaction for 22- and 13-MeV incident $^3$He.

## IV. RESULTS

### A. Spectroscopy Factors

An examination of Fig. 12 shows that the $l=3$ strength for the ($^3$He, $d$) reaction lies below 1.5 MeV excitation in $^{50}$V. Table III shows that the $l=3$ spectroscopic strength fails to exhaust the

TABLE I. DWBA input parameters for the potential

$$V(r)=V\left[f(x_R)+\frac{\lambda}{45.2}\,\frac{1}{r}\,\frac{d}{dr}f(x_R)\,\vec{L}\cdot\vec{S}\right]+i\left[W+W'\,\frac{d}{dx_i}\right]f(x_i)+V_c(r,r_c),$$

where

$$f(x_i)=\{1+\exp[(r-r_{0i}A^{1/3})/a_i]\}^{-1}.$$

| | $V$ (MeV) | $\lambda$ | $r_{0R}$ (fm) | $a_R$ (fm) | $W$ (MeV) | $W'$ (MeV) | $r_{0I}$ (fm) | $a_I$ (fm) | $r_c$ (fm) |
|---|---|---|---|---|---|---|---|---|---|
| | | | | $^{49}$Ti($^3$He, $d$)$^{50}$V | | | | | |
| $^3$He | −167.9 | 0.0 | 1.07 | 0.775 | −16.79 | | 1.611 | 0.600 | 1.4 |
| $d$ | −112 | 0.0 | 1.0 | 0.900 | 0.0 | 72 | 1.55 | 0.47 | 1.3 |
| $p$ | a | 0.0 | 1.1 | 0.65 | ··· | ··· | ··· | ··· | 1.25 |
| | | | | $^{51}$V($^3$He, $\alpha$)$^{50}$V | | | | | |
| $^3$He | −168.0 | 0 | 1.07 | 0.775 | −16.79 | 0.0 | 1.610 | 0.600 | 1.4 |
| $\alpha$ | −140.1 | 0 | 1.480 | 0.529 | −22.9 | 0.0 | 1.480 | 0.529 | 1.4 |
| $n$ | a | 25 | 1.20 | 0.65 | ··· | ··· | ··· | ··· | 1.25 |
| | | | | $^{48}$Ti($^3$He, $p$)$^{50}$V | | | | | |
| $^3$He | −173.77 | 0 | 1.14 | 0.734 | −16.21 | 0 | 1.604 | 0.753 | 1.4 |
| $p$ | −53.6 | 0 | 1.217 | 0.6 | 0 | 68.4 | 1.264 | 0.31 | 1.25 |
| $d$ | a | 0 | 1.2 | 0.65 | ··· | ··· | ··· | ··· | 1.2 |

[a] Adjusted to reproduce the experimental binding energy.

sum rule[17] by 20%, but this is the accepted error in DWBA spectroscopic factors.

The $l=1$ strength is seen to be heavily fragmented and to exhaust only 30% of the sum rule. Since the center of the strength is at about 3 MeV, it is very likely that some of the strength lies at excitation energies above 4 MeV, the upper limit of our measurement. However, much of the missing strength may lie in very many levels too weakly populated to be observed in these measurements.

Several cases in which the transferred orbital angular momentum is zero are observed in the ($^3$He, $d$) reaction. This is unexpected since the ($^3$He, $d$) reaction should not be able to populate a $2s_{1/2}$ hole state directly and the $3s_{1/2}$ state should be at too high an excitation energy to be readily populated. The shape of the angular distribution for $l=0$ transfer forces one to match the experimental data and DWBA curve at the second maximum; it is therefore possible that the $l=0$ spectroscopic strength has been severely overestimated. A small $l=0$ strength could be attributed to a $2s_{1/2}$ hole component in the $^{49}$Ti ground-state configuration.

The spectroscopic factors for the $^{51}$V($^3$He, $\alpha$)$^{50}$V reaction are plotted in Fig. 13. The measured $l=3$ strength exceeds the sum-rule limit. The total observed strength for $l=3$ is 14, whereas the sum rule predicts it to be 7.5 (Table IV). Some of this excess may be accounted for by the undistinctive shape of the angular distributions, which would allow admixtures of other $l$ values to be present but undetected so their strength would be attributed to $l=3$. However, most of the excess is probably due to the uncertainty in the normalizing constant for extracting absolute spectroscopic factors from ($^3$He, $\alpha$) absolute cross sections.

The observed $l=2$ strength does not exhaust the sum rule and very likely resides in levels above 5 MeV excitation, which were not investigated in this study. The spectroscopic strength for the $l=0$ transfer also exceeds the sum-rule limit (by ~50%) and may be due to the necessity to match the experimental and DWBA curves at the second maxima as in the corresponding case for the ($^3$He, $d$) reaction.

The ($^3$He, $p$) reaction observed at 13-MeV incident energy shows two $L_{np}=0$ angular distribu-

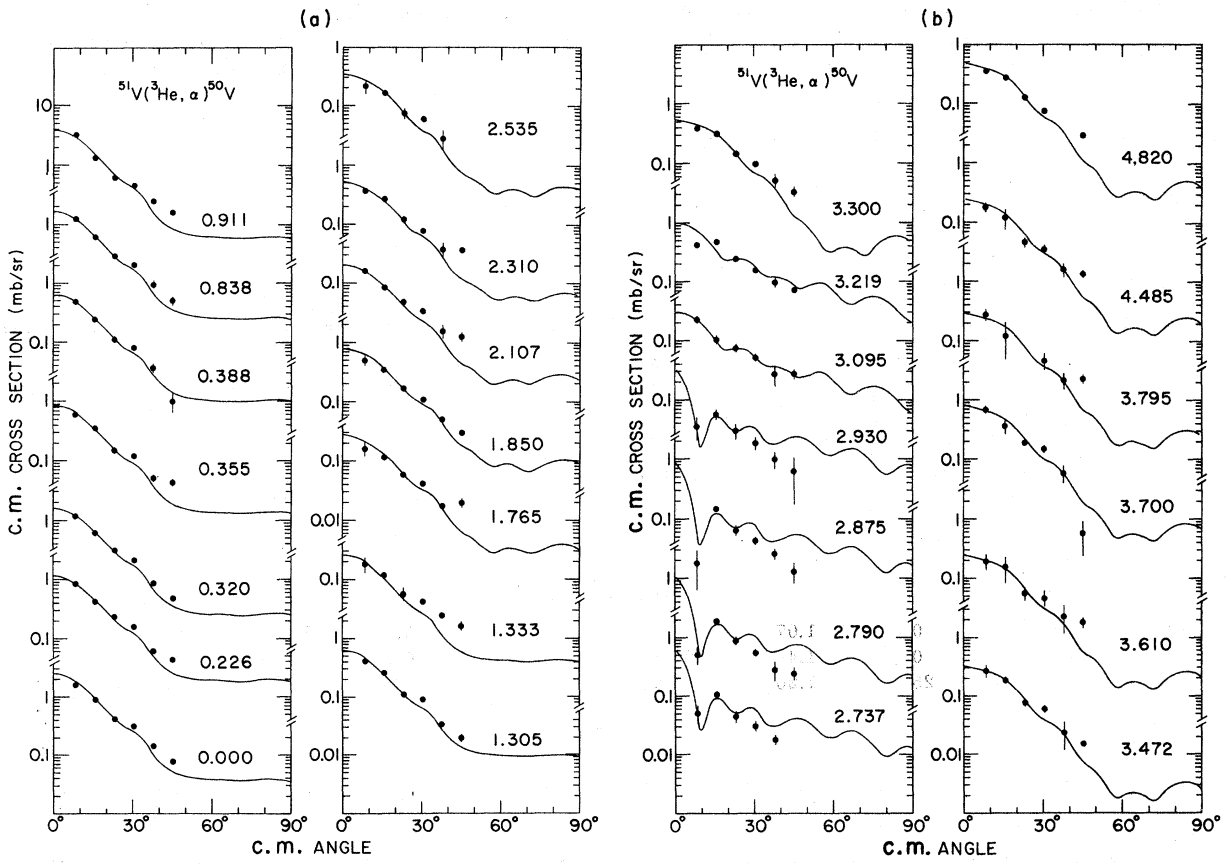


FIG. 9. Angular distributions and DWBA fits from the $^{51}$V($^3$He, $\alpha$)$^{50}$V reaction induced by 22-MeV $^3$He.

tions (Fig. 11) for transitions populating two $0^+$ analog states ($0^+ \rightarrow 0^+$ transitions). The $L_{np}=0$ distribution is distinguished by the peak at 0° followed by a deep first minimum at forward angles. A distribution with a shallower minimum than that in the pure $L_{np}=0$ shape which can be described by $L_{np}=0+2$ has shown to be associated with a $0^+ \rightarrow 1^+$ transition in the two-particle ($^3$He, $p$) transfer.[18,19] This interpretation of the angular distributions of Fig. 11 has led us to assign $J^\pi = 1^+$ to the five levels at 1.333, 1.490, 2.395, 2.819, and 3.474 MeV. Other (conclusive) evidence will be presented in Sec. V to show that two of these five levels (1.333 and 1.490 MeV) have in fact $J^\pi = 1^+$. The $\gamma$-decay work (Sec. IV B) shows the level at 3.240 MeV to be actually two closely spaced levels, hence we made no spin assignment. The distribution of the 3.575-MeV level might be $L_{np}=0$ as well as $L_{np}=0+2$. Consequently the assignment is $J^\pi = (0^+, 1^+)$.

### B. $\gamma$ Decay

In the present ($^3$He, $p\gamma$) experiment, final levels that are populated with the transfer of an $np$ pair with zero orbital angular momentum were selected preferentially by positioning the particle detector at 0°. Since the target nuclei have $J^\pi = 0^+$ ground states, final states of $J^\pi = 0^+$ or $1^+$ are preferentially populated. These low-spin states are not ex-

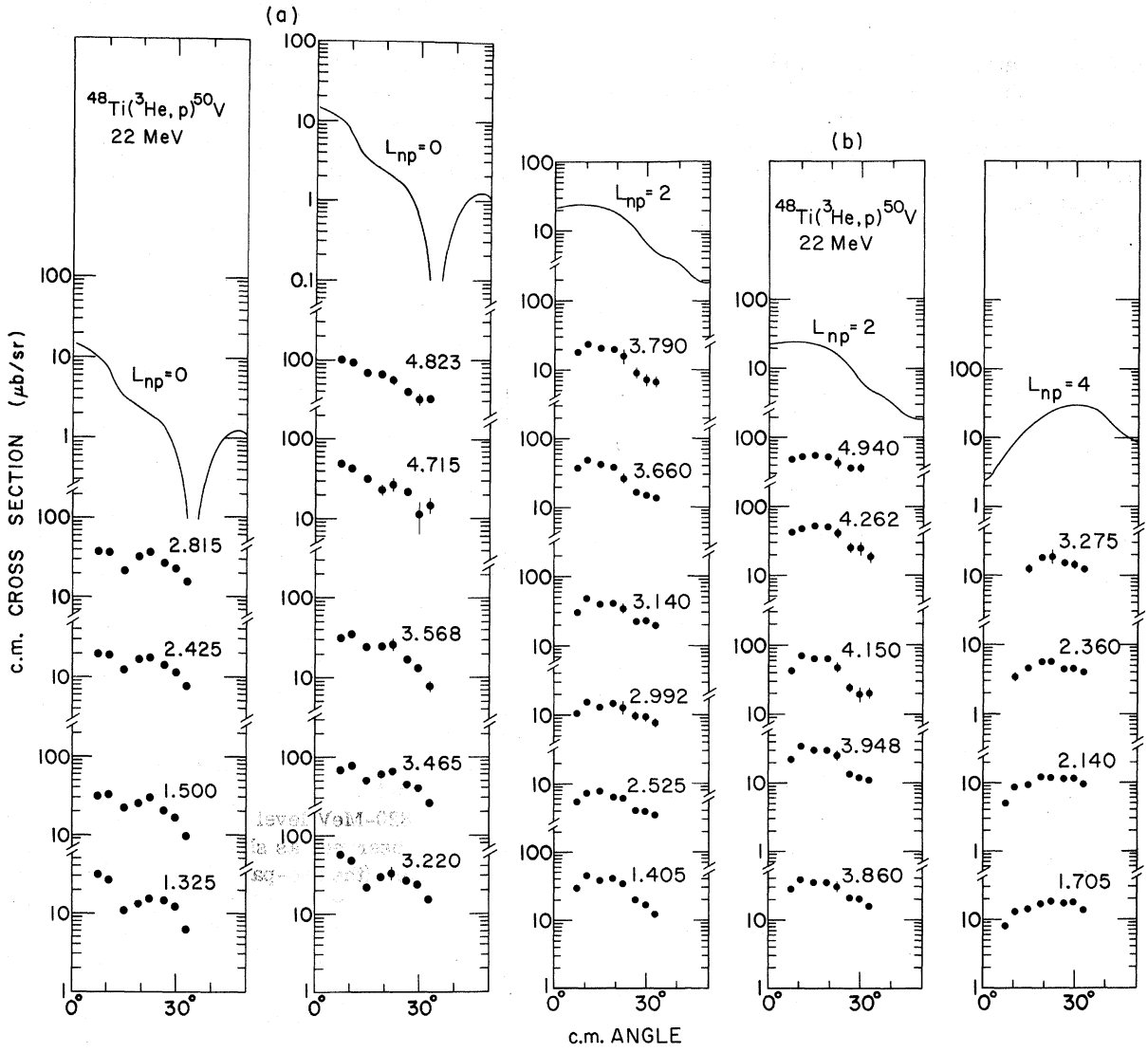


FIG. 10. Experimental and DWBA angular distributions for the $^{48}$Ti($^3$He, $p$)$^{50}$V reaction induced by 22-MeV $^3$He.

pected to decay to the lowest three states in $^{50}$V, which have $J^\pi = 4^+ - 6^+$. Instead, they are expected to seek out other low-spin states. This is observed in Fig. 3. Above 1 MeV, two states at 1.305 and 1.515 MeV (and presumably of low spin) are populated by the $\gamma$ decay of higher states but are not populated by the reaction directly.

The two $0^+$ analog states are observed to decay to only one level each. Both of the levels so populated will be established (Sec. V) to have $J^\pi = 1^+$; the $\gamma$ decay is then of $M1$ multipolarity. Other analog states in nuclei in this region of the Periodic Table are also observed to decay by $M1$ $\gamma$ transitions.[20,21]

## V. DISCUSSION

### A. Levels of $^{50}$V

#### 1. $0^+$ Analog States

The $0^+$ states at 4.820 and 8.588 MeV excitation in $^{50}$V are the analogs of the $^{50}$Ti ground state and 3.88-MeV state,[22] both of which have $J^\pi = 0^+$.

The configuration of the ground state of $^{50}$Ti is expected to be mostly $(\pi f_{7/2})^2$ plus an inert $^{48}$Ca core coupled to $J^\pi = 0^+$, $T = 3$. When $T_-$ operates on such a configuration, the result is the same inert core plus $(\pi f_{7/2})^3(\nu f_{7/2})^{-1}$ coupled to $J^\pi = 0^+$, $T = 3$. All the active nucleons still are $1f_{7/2}$. We take this as the configuration of the 4.820-MeV analog state in $^{50}$V.

The 3.88-MeV state of $^{50}$Ti, the parent of the 8.588-MeV analog state in $^{50}$V, is very likely to be a configuration in which two particles are excited to a higher shell because this state is populated with an unusually high cross section in the $(t, p)$ reaction.[8,9] Hinds *et al.*[8,9] present the ratio of the $(t, p)$ cross section for the first $0^+$ excited state in an even-even nucleus to that for its ground state as a function of its neutron number. The ratio reaches a peak at $N = 28$ ($^{50}$Ti) and then drops suddenly at $N = 30$, and we take this as evidence that the 3.88-MeV state of $^{50}$Ti represents the excitation of two $f_{7/2}$ neutrons into some mixture of the $1f_{5/2}$ and/or $2p$ orbitals (since they are almost degenerate) resulting in the configuration $(\pi 1f_{7/2})^2(\nu 1f_{7/2})^{-2}(\nu 1f_{5/2}2p)^2$ coupled to $J = 0$, $T = 3$. Operating on this wave function of the 3.88-MeV state of $^{50}$Ti with $T_-$ leads to the result that the 8.588-MeV state in $^{50}$V has the two-particle configuration

$$(\tfrac{2}{3})^{1/2}[(\pi 1f_{7/2})^3(\nu 1f_{7/2})^{-3}(\nu 1f_{5/2}2p)^2]\,{}^{T=3}_{J^\pi=0^+}$$

$$+(\tfrac{1}{3})^{1/2}[(\pi 1f_{7/2})^2(\pi 1f_{5/2}2p)(\nu 1f_{7/2})^{-2}(\nu 1f_{5/2}2p)]\,{}^{T=3}_{J^\pi=0^+}\,.$$

If indeed the dominant configurations of the two analog states are as indicated, then both analog states should be strongly populated in the ($^3$He, $p$) reaction. This is observed in Fig. 6 (peaks 93 and 110) and in Fig. 7 (peak 93).

The two analog states may also be studied by one-particle-transfer reactions. If the ground state of the $^{49}$Ti target is assumed to be wholly $1f_{7/2}$ configuration, then the ($^3$He, $d$) reaction should populate the 4.820-MeV state by $l_p = 3$ transfer but not the state at 8.588 MeV. The 4.820-MeV level is seen (Fig. 4, peak 93), but contaminants in the target prevent the determination of an angular distribution to certify that the proton is transferred with $l_p = 3$. No ($^3$He, $d$) measurement was made at 8.58 MeV excitation. The ($^3$He, $\alpha$) reaction, like the ($^3$He, $d$), should populate the 4.820-MeV level by $l_n = 3$ transfer. This is indeed observed, as shown in Fig. 9. The level at 8.588 MeV (the two-particle excitation) should not be strongly populated in ($^3$He, $\alpha$) reactions; it is in fact not observed in a $^{51}$V($^3$He, $\alpha$)$^{50}$V spectrum at 26° and 13-MeV bombarding energy.[23]

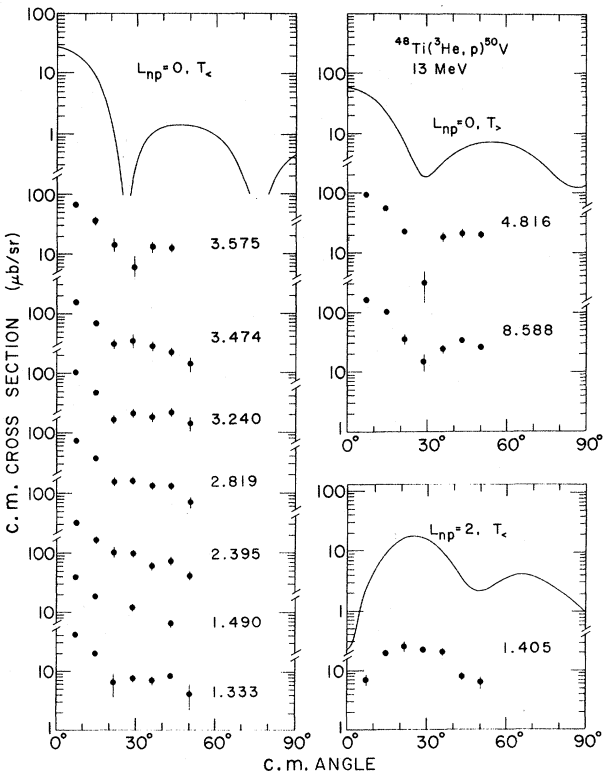


FIG. 11. Experimental and DWBA angular distributions for the $^{48}$Ti($^3$He, $p$)$^{50}$V reaction induced by 13-MeV $^3$He.

#### 2. $1^+$ Levels at 1.333 and 1.490 MeV

The levels at 1.333 and 1.490 MeV are populated by the $\gamma$ decay (Fig. 3) of the 4.820- and

TABLE II. Experimental data on $^{50}$V.

| Level No. | $^{50}$V$(p,p')^{50}$V [a] $E_x$ (MeV) | $^{49}$Ti$(^3$He$,d)^{50}$V [b] $E_x$ (MeV) | $l_p$ | $^{49}$Ti$(^3$He$,d)^{50}$V [c] $E_x$ (MeV) | $l_p$ | $\frac{2J_f+1}{2J_i+1}S$ | $^{51}$V$(d,t)^{50}$V [d] $E_x$ (MeV) | $l_n$ | $S_{I=3}$ |
|---|---|---|---|---|---|---|---|---|---|
| 1 | 0.0 | 0.0 | 3 | 0.0 | 3 | 0.91 | 0.0 | 1+3 | 1.57 |
| 2 | 0.226 | 0.226 | 1+3 | 0.226 | 1+3 | 0.23+0.38 | 0.228 | 1+3 | 0.66 |
| 3 | 0.321 | 0.318 | 3 | 0.320 | 3 | 0.60 | 0.321 | 1+3 | 0.99 |
| 4 | 0.358 | 0.350 | 1+3 | 0.355 | 3 | 0.55 | 0.357 | 1+3 | 0.56 |
| 5 | 0.390 | 0.388 | 3 | 0.388 | 1+3 | 0.01+0.38 | 0.387 | 1+3 | 0.32 |
| 6 | 0.838 | 0.836 | | 0.838 | 1+3 | 0.01+0.36 | 0.838 | 1+3 | 1.01 |
| 7 | 0.911 | 0.911 | 3 | 0.911 | 3 | 1.3 | 0.911 | 1+3 | 2.67 |
| 8 | 1.305 | 1.307 | 1+3 | 1.305 | 1+3 | 0.005+0.18 | 1.301 | 1+3 | 0.33 |
| 9 | 1.330 | 1.347 | 1+3 | 1.333 | 3 | 0.25 | 1.330 | 1+3 | 0.23 |
| 10 | 1.404 | | | | | | 1.402 | 1 | |
| 11 | | | | | | | | | |
| 12 | 1.519 | | | 1.515 | | | | | |
| 13 | 1.561 | | | | | | | | |
| 14 | 1.701 | | | | | | | | |
| 15 | 1.725 | | | | | | | | |
| 16 | 1.753 | | | | | | | | |
| 17 | 1.760 | | | 1.757 | | | | | |
| 18 | 1.808 | | | 1.810 | | | | | |
| 19 | 1.884 | | | | | | | | |
| 20 | 1.937 | | | | | | | | |
| 21 | 1.957 | | | | | | | | |
| 22 | 2.038 | | | 2.030 | | | | | |
| 23 | 2.112 | | | 2.110 | 1 | 0.02 | | | |
| 24 | 2.133 | | | | | | | | |
| 25 | 2.162 | | | 2.115 | | | | | |
| 26 | 2.314 | 2.300 | 1 | 2.300 | 1 | 0.04 | | | |
| 27 | 2.342 | 2.348 | 1 | 2.350 | 1 | 0.13 | | | |
| 28 | 2.399 | | | | | | | | |
| 29 | 2.422 | 2.427 | 0 | 2.420 | 0 | 0.22 | | | |
| 30 | 2.456 | 2.467 | 1 | 2.460 | 1 | 0.11 | | | |
| 31 | 2.481 | | | | | | | | |
| 32 | 2.492 | | | 2.495 | | | | | |
| 33 | 2.512 | | | | | | | | |
| 34 [g] | 2.533 | 2.542 | 0 | 2.535 | 0 | 0.17 | | | |
| 35 | 2.600 | | | 2.595 | | | | | |
| 36 | 2.655 | 2.658 | 1 | 2.650 | 1 | 0.05 | | | |
| 37 | 2.738 | | | | | | | | |
| 38 | 2.763 | | | | | | | | |
| 39 | 2.792 | | | | | | | | |
| 40 | 2.815 | 2.814 | | 2.810 | 1 | 0.013 | | | |
| 41 | 2.828 | | | | | | | | |
| 42 | 2.849 | | | | | | | | |
| 43 | | | | | | | | | |
| 44 | 2.931 | | | | | | | | |
| 45 | 2.958 | | | | | | | | |
| 46 | 2.965 | 2.966 | 1+3 | 2.960 | 1 | 0.07 | | | |
| 47 | 2.992 | 2.996 | | 2.990 | 1 | 0.022 | | | |
| 48 | 3.011 | | | | | | | | |
| 49 | 3.099 | 3.101 | 1 | 3.100 | 1 | 0.02 | | | |
| 50 | | | | | | | | | |
| 51 | 3.111 | | | | | | | | |
| 52 | 3.142 | 3.140 | | 3.138 | 1 | 0.05 | | | |
| 53 | 3.169 | | | | | | | | |
| 54 [h] | 3.202 | | | | | | | | |
| 55 | | | | 3.255 | 1 | 0.02 | | | |
| 56 | 3.274 | | | | | | | | |
| 57 | 3.297 | 3.285 | | 3.295 | 1 | 0.2 | | | |
| 58 | 3.312 | | | | | | | | |
| 59 | 3.433 | | | | | | | | |

TABLE II. Experimental data on $^{50}$V.

| Level No. | $^{51}$V($^3$He, $\alpha$)$^{50}$V [e] $E_x$ (MeV) | $l_n$ | $S$ | $^{48}$Ti($^3$He, $p$)$^{50}$V [f] 22 MeV $E_x$ (MeV) | $L_{np}$ | $\left(\frac{d\sigma}{d\Omega}\right)_{max}$ ($\mu$b/sr) | 13 MeV $E_x$ (MeV) | $L_{np}$ | $\left(\frac{d\sigma}{d\Omega}\right)_{max}$ ($\mu$b/sr) | $J^\pi$ |
|---|---|---|---|---|---|---|---|---|---|---|
| 1 | 0.0 | 3 | 1.9 | | | | | | | $6^+$ |
| 2 | 0.226 | 3 | 0.9 | | | | | | | $(5^+)$ |
| 3 | 0.320 | | 1.3 | | | | | | | $(4^+)$ |
| 4 | 0.355 | 3 | 0.7 | | | | | | | $(3^+)$ |
| 5 | 0.388 | 3 | 0.5 | | | | | | | $(2^+)$ |
| 6 | 0.838 | 3 | 1.3 | | | | | | | |
| 7 | 0.911 | 3 | 3.1 | | | | | | | $7^+$ |
| 8 | 1.305 | 3 | 0.5 | | | | | | | |
| 9 | 1.333 | 3 | 0.2 | 1.325 | 0+2 | 31 | 1.333 | 0+2 | 41 | $1^+$ |
| 10 | | | | 1.405 | 2 | 45 | 1.405 | 2 | 25 | |
| 11 | | | | 1.500 | 0+2 | 32 | 1.490 | 0+2 | 39 | $1^+$ |
| 12 | 1.515 | | | | | | | | | |
| 13 | | | | 1.570 | | | | | | |
| 14 | 1.710 | | | | | | | | | |
| 15 | | | | | | | | | | |
| 16 | | | | 1.750 | 4 | 18 | | | | |
| 17 | 1.765 | 3 | 0.2 | | | | | | | |
| 18 | | | | | | | | | | |
| 19 | | | | | | | | | | |
| 20 | | | | | | | | | | |
| 21 | 1.950 | 3 | 0.6 | 1.950 | | | | | | |
| 22 | 2.040 | | | | | | | | | |
| 23 | 2.107 | 3 | 0.11 | | | | | | | |
| 24 | | | | 2.140 | 4 | 12 | | | | |
| 25 | 2.150 | | | | | | | | | |
| 26 | 2.310 | 3 | 0.3 | | | | | | | |
| 27 | 2.350 | | | 2.360 | 4 | 6 | | | | |
| 28 | | | | 2.425 | 0+2 | 20 | 2.395 | 0+2 | 34 | $1^+$ |
| 29 | 2.422 | | | | | | | | | |
| 30 | 2.460 | | | | | | | | | |
| 31 | | | | | | | | | | |
| 32 | | | | | | | | | | |
| 33 | | | | | | | | | | |
| 34 [g] | 2.535 | 3 | 0.2 | 2.525 | 2 | 8 | | | | |
| 35 | 2.595 | | | | | | | | | |
| 36 | 2.645 | | | | | | | | | |
| 37 | 2.737 | 0 | 0.5 | | | | | | | |
| 38 | | | | | | | | | | |
| 39 | | | | | | | | | | |
| 40 | 2.790 | 0 | 0.9 | | | | | | | |
| 41 | | | | 2.815 | 0+2 | 37 | 2.819 | 0+2 | 75 | $1^+$ |
| 42 | | | | | | | | | | |
| 43 | 2.875 | 0 | 0.7 | | | | | | | |
| 44 | 2.930 | 0 | 0.3 | | | | | | | |
| 45 | | | | | | | | | | |
| 46 | | | | | | | | | | |
| 47 | 2.985 | | | 2.992 | 2 | 15 | | | | |
| 48 | | | | | | | | | | |
| 49 | | | | | | | | | | |
| 50 | 3.095 | 2 | 0.4 | | | | | | | |
| 51 | | | | | | | | | | |
| 52 | 3.135 | | | 3.140 | 2 | 45 | | | | |
| 53 | | | | | | | | | | |
| 54 [h] | 3.219 | 2 | 1.3 | 3.220 | 0 | 56 | 3.240 | 0 | 105 | |
| 55 | | | | | | | | | | |
| 56 | | | | 3.275 | 4 | 19 | | | | |
| 57 | | | | | | | | | | |
| 58 | 3.300 | 3 | 0.4 | | | | | | | |
| 59 | | | | | | | | | | |

TABLE II *(Continued)*

| Level No. | $^{50}V(p,p')^{50}V$ [a] $E_x$ (MeV) | $^{49}Ti(^3He,d)^{50}V$ [b] $E_x$ (MeV) | $l_p$ | $^{49}Ti(^3He,d)^{50}V$ [c] $E_x$ (MeV) | $l_p$ | $\frac{2J_f+1}{2J_i+1}S$ | $^{51}V(d,t)^{50}V$ [d] $E_x$ (MeV) | $l_n$ | $S_{I=3}$ |
|---|---|---|---|---|---|---|---|---|---|
| 60 | 3.482 | | | | | | | | |
| 61 | | 3.537 | | 3.540 | 1 | 0.056 | | | |
| 62 [i] | 3.566 | | | | | | | | |
| 63 | | | | 3.595 | | | | | |
| 64 | 3.671 | | | 3.655 | | | | | |
| 65 | 3.700 | 3.713 | | 3.700 | 1 | 0.02 | | | |
| 66 | 3.722 | | | | | | | | |
| 67 | 3.730 | | | | | | | | |
| 68 | 3.749 | | | | | | | | |
| 69 | | 3.813 | 1 | 3.813 | 1 | 0.047 | | | |
| 70 | | | | | | | | | |
| 71 | | 3.885 | 1 | 3.883 | 1 | 0.028 | | | |
| 72 | | 3.939 | 1 | 3.915 | 1 | 0.01 | | | |
| 73 | | | | 3.955 | 1 | 0.01 | | | |
| 74 | | | | | | | | | |
| 75 | | 4.081 | 1 | 4.080 | 1 | 0.027 | | | |
| 76 | | 4.124 | | 4.115 | | | | | |
| 77 | | 4.151 | 1 | 4.150 | 1 | 0.065 | | | |
| 78 | | 4.213 | | | | | | | |
| 79 | | | | | | | | | |
| 80 | | 4.282 | | | | | | | |
| 81 | | | | | | | | | |
| 82 | | 4.407 | | | | | | | |
| 83 | | | | | | | | | |
| 84 | | 4.441 | | | | | | | |
| 85 | | | | | | | | | |
| 86 | | 4.513 | | | | | | | |
| 87 | | | | | | | | | |
| 88 | | 4.581 | | | | | | | |
| 89 | | 4.602 | | | | | | | |
| 90 | | 4.664 | | 4.650 | | | | | |
| 91 | | | | | | | | | |
| 92 | | 4.774 | | | | | | | |
| 93 [j] | | 4.833 | | 4.820 | | | | | |
| 94 | | 4.898 | | | | | | | |
| 95 | | 4.928 | | 4.920 | | | | | |
| 96 | | 5.018 | | | | | | | |
| 97 | | 5.058 | | 5.070 | | | | | |
| 98 | | 5.090 | | | | | | | |
| 99 | | 5.326 | | | | | | | |
| 100 | | 5.409 | | | | | | | |
| 101 | | 5.531 | | | | | | | |
| 102 | | 5.645 | | | | | | | |
| 103 | | 5.755 | | | | | | | |
| 104 | | 5.786 | | | | | | | |
| 105 | | 5.820 | | | | | | | |
| 106 | | 5.893 | | | | | | | |
| 107 | | 5.951 | | | | | | | |
| 108 | | | | | | | | | |
| 109 | | | | | | | | | |
| 110 [j] | | | | | | | | | |
| 111 | | | | | | | | | |
| 112 | | | | | | | | | |

[a] Reference 7.
[b] Reference 3.
[c] This work. The quantity $[(2J_f+1)/(2J_i+1)]S$ was calculated on the assumption that $J=l+\frac{1}{2}$ for the transferred proton.
[d] Reference 6.
[e] This work. $S$ was calculated on the assumption that $J=l+\frac{1}{2}$ for the transferred neutron.
[f] This work. $L_{np}$ values indicate the major component.
[g] Two closely spaced levels with quite different nucleon configurations as shown by their population with the listed particle reactions.

TABLE II *(Continued)*

| Level No. | $^{51}$V($^3$He, $\alpha$)$^{50}$V [e] $E_x$ (MeV) | $l_n$ | $S$ | $^{48}$Ti($^3$He, $p$)$^{50}$V [f] 22 MeV $E_x$ (MeV) | $L_{np}$ | $\left(\frac{d\sigma}{d\Omega}\right)_{max}$ ($\mu$b/sr) | 13 MeV $E_x$ (MeV) | $L_{np}$ | $\left(\frac{d\sigma}{d\Omega}\right)_{max}$ ($\mu$b/sr) | $J^\pi$ |
|---|---|---|---|---|---|---|---|---|---|---|
| 60 | 3.472 | 3 | 0.2 | 3.465 | 0+2 | 77 | 3.474 | 0+2 | 155 | $1^+$ |
| 61 | | | | | | | | | | |
| 62 [i] | | | | 3.568 | 0;0+2 | 35 | 3.575 | 0;0+2 | 68 | $0^+,1^+$ |
| 63 | 3.610 | 3 | 0.2 | | | | | | | |
| 64 | | | | 3.660 | 2 | 49 | | | | |
| 65 | 3.700 | 3 | 0.6 | | | | | | | |
| 66 | | | | | | | | | | |
| 67 | | | | | | | | | | |
| 68 | 3.795 | 3 | 0.2 | 3.790 | 2 | 23 | 3.790 | | | |
| 69 | | | | | | | | | | |
| 70 | 3.840 | | | | | | | | | |
| 71 | 3.885 | | | 3.860 | 2 | 38 | 3.870 | | | |
| 72 | | | | | | | | | | |
| 73 | 3.950 | | | 3.948 | 2 | 34 | | | | |
| 74 | 4.035 | | | | | | | | | |
| 75 | 4.095 | | | 4.072 | | | | | | |
| 76 | 4.137 | | | | | | | | | |
| 77 | | | | 4.150 | 2 | 69 | 4.145 | | | |
| 78 | | | | | | | | | | |
| 79 | 4.240 | | | 4.262 | 2 | 50 | 4.245 | | | |
| 80 | 4.300 | | | | | | | | | |
| 81 | 4.340 | | | 4.345 | | | | | | |
| 82 | 4.395 | | | | | | | | | |
| 83 | 4.430 | | | 4.427 | | | | | | |
| 84 | | | | | | | 4.445 | | | |
| 85 | 4.485 | 3 | 0.2 | | | | | | | |
| 86 | | | | | | | | | | |
| 87 | 4.555 | | | 4.562 | | | | | | |
| 88 | 4.585 | | | | | | | | | |
| 89 | 4.615 | | | | | | | | | |
| 90 | | | | | | | | | | |
| 91 | | | | 4.715 | 0 | 49 | 4.720 | | | |
| 92 | 4.770 | | | | | | | | | |
| 93 [j] | 4.820 | 3 | 0.37 | 4.823 | 0 | 95 | 4.816 | 0 | 98 | $0^+$ |
| 94 | | | | | | | | | | |
| 95 | | | | 4.940 | 2 | 55 | | | | |
| 96 | | | | | | | | | | |
| 97 | | | | 5.042 | | | | | | |
| 98 | | | | | | | | | | |
| 99 | | | | | | | | | | |
| 100 | | | | | | | | | | |
| 101 | | | | | | | | | | |
| 102 | | | | | | | | | | |
| 103 | | | | | | | | | | |
| 104 | | | | | | | | | | |
| 105 | | | | | | | | | | |
| 106 | | | | | | | | | | |
| 107 | | | | | | | | | | |
| 108 | | | | | | | 6.560 | | | |
| 109 | | | | | | | 6.610 | | | |
| 110 [j] | | | | | | | 8.588 | 0 | 160 | $0^+$ |
| 111 | | | | | | | 9.115 | | | |
| 112 | | | | | | | 9.164 | | | |

[h] Two levels are populated, but not resolved, with the ($^3$He, $p$) reaction. They are resolved in the ($^3$He, $p\gamma$) study. A third level, at 3.219 MeV, has a different nucleon configuration from the above two levels, as indicated by its population with $l_n = 2$ in the ($^3$He, $\alpha$) reaction.

[i] Tentatively assigned as a $0^+$ antianalog state by T. Caldwell [quoted by Ole Hansen and C. Nathan, Phys. Rev. Letters 27, 1810 (1971)].

[j] Isobaric analog state.

8.588-MeV $J=0$ analog states, respectively, and hence cannot be $J=0$ themselves. Further, they are strongly populated in the $^{48}$Ti($^3$He, $p$)$^{50}$V reaction with predominately $L_{np}=0$ momentum transfer, which allows a spin assignment of only $J^\pi=0^+$ or $1^+$. These states are then $J^\pi=1^+$. From the preceding discussion of the nature of the analog states at 4.820 and 8.588 MeV and the fact that their respective $\gamma$ decays to the 1.333- and 1.490-MeV states are $M1$, one can draw some conclusions about the nature of these latter states.

In such a pronounced $M1$ transition, it is reasonable to assume that there is no change in the orbitals of the particles making the transition. Therefore one can conclude that the configuration of the 1.333-MeV state is wholly $f_{7/2}$. (Some $f_{5/2}$ components would be possible but unlikely.) With this configuration then, this level should be strongly populated by the ($^3$He, $d$) and ($^3$He, $\alpha$) reactions with three units of orbital angular momentum. This is indeed observed (Figs. 4 and 5 and Table II). It is then very likely that this $1^+$ level has a large component of the $1^+$ member of the $(\pi f_{7/2})(\nu f_{7/2})^{-1}$ octet, which is expected at a few MeV in analogy with a similar component in $^{48}$Sc.[24]

The configuration of the level at 8.588 MeV was shown to have two particles excited into the $(1f_{5/2}2p)$ shell. Again the 8.588- and 1.490-MeV states are connected through an $M1$ transition. By the reasoning of the previous paragraph, it is reasonable to conclude that the configuration of the 1.490-MeV state also contains two particles excited to the $(1f_{5/2}2p)$ orbitals. If this is the case, then one does not expect this state to be populated by the ($^3$He, $d$) nor ($^3$He, $\alpha$) reactions studied here (and indeed it is not seen in Figs. 4 and 5) nor in the $^{50}$V($p, p'$)$^{50}$V studied by Buhl *et al.*[7] The 1.490-MeV level is indeed unobserved in all these reactions, and we take it to be a low-lying $1^+$ with a significant admixture of two-particle configration.

### 3. *$2^+$ Level at 0.388, $3^+$ at 0.355, $4^+$ at 0.322, $5^+$ at 0.226, and $6^+$ at 0.000 MeV*

The fact that the ($^3$He, $d$) and ($^3$He, $\alpha$) reactions reported in this work have populated the low levels with a large $l=3$ spectroscopic factor (Table II) implies that they are mostly $1f_{7/2}$ configuration, though a very small admixture of $l=1$ transfer was observed in the ($^3$He, $d$) reaction to some final states. Unfortunately, the spins of these levels cannot be extracted from the spectroscopic factors because this factor is strongly affected by the specific nucleon configuration (even for wholly $1f_{7/2}$ nucleons). However, the results of the ($^3$He, $p$) and ($^3$He, $p\gamma$) measurements tend to support the assigned spins.[4,16] The ($^3$He, $p$) reaction with angular momentum transfer $L_{np}=0$ should not populate levels with $J^\pi \geq 2^+$, and these low levels are not in fact observed to be populated. However, the ($^3$He, $p$) reaction would populate a $J^\pi=1^+$, $1f_{7/2}$ configuration (as it does for the level at 1.333 MeV), so that probably none of these levels are $1^+$. The $\gamma$ decay of the high-lying $0^+$ or $1^+$ levels populated by ($^3$He, $p$) with momentum transfer $L_{np}=0$ is expected to proceed to levels with $J=0-2$; and we see (Fig. 3) that only the $(2^+)$ level at 0.388 MeV is populated by the $\gamma$ decay, not the lower levels ($J^\pi \geq 3^+$). On the basis of this evidence, the five lowest levels in $^{50}$V are assigned as the $2^+-6^+$ members of the $(\pi f_{7/2})(\nu f_{7/2}^{-1})$ octet.

### 4. *Levels of Odd Parity*

Six levels populated by the ($^3$He, $\alpha$) are seen (Table II) to proceed by a transfer of $l=0$ or 2. These states at 2.737, 2.790, 2.875, 2.930, 3.095, and 3.219 MeV have large spectroscopic strengths (Table IV) and are taken as levels with $2s_{1/2}$ or $1d_{3/2}$ hole configurations. As expected these levels are not populated by the ($^3$He, $p$) reaction. For this reason the two states at about 3.230 MeV, seen in the ($^3$He, $p$) reaction, are not the same as the 3.219-MeV state seen in the ($^3$He, $\alpha$) reaction.

## B. Comparison with Nuclear Models

The wave functions calculated by MBZ[1] for nuclei having only $1f_{7/2}$ active nucleons may be used to calculate the spectroscopic factors of the $^{49}$Ti-($^3$He, $d$)$^{50}$V and $^{51}$V($^3$He, $\alpha$)$^{50}$V reactions for those final states predicted by the model. The values are listed in Table III, and further details can be found in Ref. 10. (Note also that some of the calculated spectroscopic factors published in Ref. 3 are incorrect.) The experimental spectroscopic factors and the MBZ predictions for reactions populating states in $^{50}$V are compared in Fig. 14 for proton stripping and in Fig. 15 for neutron pickup.

From either figure, one sees that the theoretical energy levels agree with the observed ones up to about 1 MeV. The theory predicts extra $4^+$ and $5^+$ states near the level seen at 838 keV. It is not clear which, if either, of these states corresponds to the experimental level. Above 1.0–1.5 MeV, the MBZ predictions are not meaningful because there are increasing admixtures of the $2p$ configuration. The exception to this is the $0^+$ analog state for which an excitation energy of 4.645 MeV and a pure $f_{7/2}$ configuration are predicted. It is actually observed at 4.820 MeV.

The theoretical spectroscopic factors for proton stripping (Fig. 14) agree with those measured in

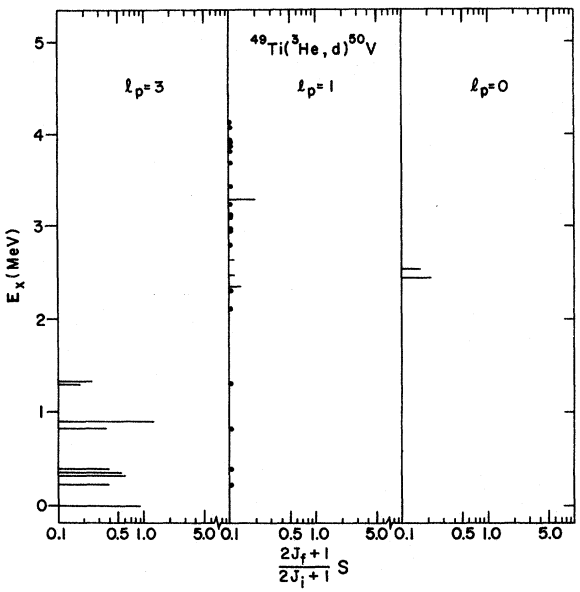


FIG. 12. The spectroscopic factors obtained from a DWBA analysis of the data on the $^{49}$Ti($^3$He, $d$)$^{50}$V reaction. The results for $l_p$=3, 1, and 0 are plotted as a function of excitation energy. Dots indicate factors less than 0.1.

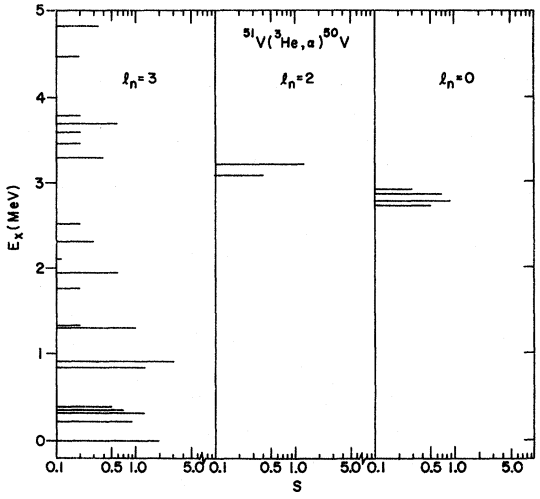


FIG. 13. The spectroscopic factors obtained from a DWBA analysis of the data on the $^{51}$V($^3$He, $\alpha$)$^{50}$V reaction. Results for $l_n$=3, 2, and 0 are indicated by the length of the bar at the appropriate excitation energy.

TABLE III. MBZ spectroscopic factors.

| | | ($^3$He, $d$) | | | | ($^3$He, $d$) | |
|---|---|---|---|---|---|---|---|
| $E_x$ (MeV) | $I(T_<)$ | $\frac{2J_f+1}{2J_i+1}S$ | ($^3$He, $\alpha$) $S$ | $E_x$ (MeV) | $I(T_<)$ | $\frac{2J_f+1}{2J_i+1}S$ | ($^3$He, $\alpha$) $S$ |
| 1.5811 | 1 | 0.249 67 | 0.140 36 | 0.0000 | 6 | 1.065 61 | 1.145 80 |
| 2.950 | 1 | 0.038 19 | 0.067 16 | 2.0335 | 6 | 0.011 05 | 0.109 51 |
| 4.2158 | 1 | 0.121 38 | 0.167 43 | 3.3129 | 6 | 0.000 44 | 0.077 79 |
| | | | | 4.3418 | 6 | 0.000 14 | 0.111 46 |
| 0.3197 | 2 | 0.556 30 | 0.457 96 | | | | |
| 1.6144 | 2 | 0.011 67 | 0.056 89 | 1.2104 | 7 | 1.680 01 | 1.698 25 |
| 2.8483 | 2 | 0.000 40 | 0.008 37 | 2.6533 | 7 | 0.008 96 | 0.084 35 |
| 4.7346 | 2 | 0.000 11 | 0.032 29 | 3.8585 | 7 | 0.000 48 | 0.046 69 |
| | | | | 5.9291 | 7 | 0.000 19 | 0.045 63 |
| 0.0347 | 3 | 0.533 15 | 0.394 20 | | | | |
| 2.0748 | 3 | 0.080 34 | 0.254 39 | 1.9521 | 8 | 0.0 | 0.0 |
| 2.8265 | 3 | 0.032 27 | 0.130 98 | 3.7164 | 8 | 0.0 | 0.0 |
| 3.2223 | 3 | 0.018 97 | 0.065 12 | 4.1531 | 8 | 0.0 | 0.0 |
| 5.5033 | 3 | 0.004 55 | 0.030 27 | | | | |
| | | | | 2.8601 | 9 | 0.0 | 0.0 |
| 0.1078 | 4 | 0.292 65 | 0.271 44 | 4.4192 | 9 | 0.0 | 0.0 |
| 0.8849 | 4 | 0.390 89 | 0.675 53 | | | | |
| 2.3402 | 4 | 0.002 42 | 0.003 76 | 4.6291 | 10 | 0.0 | 0.0 |
| 3.3368 | 4 | 0.001 34 | 0.004 25 | | | | |
| 5.7210 | 4 | 0.000 07 | 0.045 04 | 4.9049 | 11 | 0.0 | 0.0 |
| | | | | | $I(T_>)$ | | |
| 0.2248 | 5 | 0.439 33 | 0.535 39 | 4.6447 | 0 | 0.139 00 | 0.125 00 |
| 0.8676 | 5 | 0.304 27 | 0.639 17 | | | | |
| 2.3367 | 5 | 0.001 03 | 0.000 10 | 6.1537 | 2 | 0.027 44 | 0.069 40 |
| 3.1923 | 5 | 0.000 04 | 0.076 19 | 2.6427 | 4 | 0.000 06 | 0.125 00 |
| 4.8217 | 5 | 0.000 49 | 0.118 36 | | | | |
| 6.5980 | 5 | 0.000 00 | 0.005 76 | 8.0447 | 6 | 0.000 04 | 0.180 00 |

the present work and, except for the 0.838-MeV level, with those from Ref. 3. The agreement with Ref. 3 is due to the use of different optical-model potentials, since the absolute cross sections were not consistent (Sec. II B). Although Bishop, Pullen, and Rosner[3] called the 0.838-MeV level a "non-stripping" one, our data (Fig. 10) show a stripping pattern. The spectroscopic factors for the $6^+$ ground state, the $5^+$ at 0.226 MeV, the $7^+$ at 0.911 MeV, and the $1^+$ at 1.333 MeV are well reproduced by the MBZ theory, and the agreement is acceptable for the $3^+$ state at 0.322 MeV, the $4^+$ at 0.355 MeV, and the $2^+$ at 0.388 MeV.

The spectroscopic factors for neutron pickup reactions are shown in Fig. 15. The relative values from the present measurement agree with those from other experiments.[6,26] The MBZ predictions are in good agreement for the ground state and the 0.226- and 0.911-MeV states, and the agreement is acceptable for the 0.322-, 0.355-, 0.388-, and 1.333-MeV states.

The Coriolis-coupling model of Malik and Scholz[27,28] has been applied to the odd-$A$ nuclei in the $1f_{7/2}$ shell with considerable success. The model has recently been extended to odd-odd nuclei by Wasielewski and Malik[29] and has had some success in the $1f$-$2p$ shell.[30] These calculations are readily carried out for $^{50}$V and are discussed in detail in Ref. 10.

TABLE IV. Sums of spectroscopic factors.

| Assumed orbital | $^{49}$Ti($^3$He, $d$)$^{50}$V $\sum \frac{2J_f+1}{2J_i+1} S(T_<)$ | Sum-rule limit [a] | $^{51}$V($^3$He, $\alpha$)$^{50}$V $\sum S(T_<)$ | Sum-rule limit [a] |
|---|---|---|---|---|
| $2s_{1/2}$ | 0.39 [b] | 0 | 2.4 [b] | 1.667 |
| $1d_{3/2}$ | 0 | 0 | 1.8 | 3.333 |
| $1f_{7/2}$ | 4.91 | 5.833 | 14 | 7.500 |
| $2p_{3/2}$ | 1.06 | 3.333 | 0 | 0 |

[a] French and Macfarlane, Ref. 17.
[b] DWBA calculation matched to experimental data at the second maximum.

Figure 16 compares the experimental energy levels, the predictions of MBZ, and three energy-level schemes in the Coriolis-coupling model with different values of the deformation parameter $\beta$ and core-softening parameter $Q$ (as discussed in Refs. 2 and 10). The energy of the ground state has a broad minimum in the region $-0.2 \leq \beta \leq -0.3$. We take it as fortuitous that the best energy-level schemes are obtained near $Q=1$, where the core is unaffected by the states of the two particles outside the core, as would be expected in the simplest model.

The levels in the Coriolis-coupling model are seen to be compressed relative to either the ex-

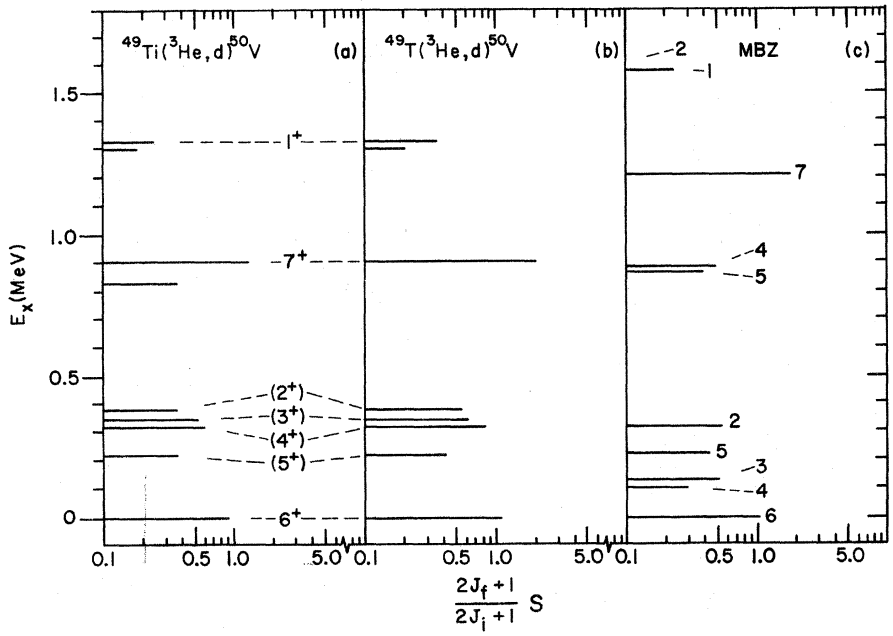


FIG. 14. Spectroscopic factors obtained (a) from the present work and (b) from the measurements of Bishop, Pullen, and Rosner (Ref. 3) by DWBA analysis of data on proton stripping in the $^{49}$Ti($^3$He,$d$) reaction to states in $^{50}$V and (c) from calculations by use of the MBZ theory. The length of the bar indicates the spectroscopic factor for the state at the excitation energy shown.

perimental data or the MBZ prediction. This compression is observed for all the parameter sets we have tried. Interestingly, we observe an extra $4^+$, $5^+$ pair in the Coriolis-coupling calculations, just as in the MBZ calculations. Two low-lying $1^+$ levels, possibly corresponding to the $1^+$ levels at 1.333 and 1.490 MeV, are produced in the Coriolis-coupling calculation; but only one is produced in the MBZ calculation, as expected since the latter assumes a pure $f_{7/2}$ configuration.

No attempt was made to calculate the spectroscopic factors from the wave functions provided by the Coriolis-coupling model for odd-odd nuclei. However, some electromagnetic moments were calculated. The ground-state magnetic dipole moment[31] can be reproduced with the wave function of a lowest $6^+$ level.

## VI. SUMMARY AND CONCLUSIONS

Spectroscopic factors were extracted by means of DWBA analyses of the angular distributions of proton-stripping and neutron-pickup reactions to $^{50}$V. The DWBA analysis of the ($^3$He, $p$) reaction has allowed the assignment of angular momentum transfers $L_{np}$ for this reaction, but no spectroscopic factors could be extracted.

This work has resulted in assigning $J^\pi = 1^+$ to the 1.333- and 1.490-MeV levels of $^{50}$V. The level at 1.490 MeV is seen to be a two-particle excited state with two nucleons in the degenerate $1f_{5/2}$ and $2p$ orbitals, whereas the 1.333-MeV level is purely $1f_{7/2}$. The spins of the lowest four excited states had been tentatively assigned by other authors,[4,16] and our measurements support the suggested assignments. These four states of spin $2^+$–$5^+$, along with the $6^+$ ground state, the $7^+$ state at 0.911 MeV, and the $1^+$ state at 1.333 MeV, are assumed to belong to the $(\pi f_{7/2})(\nu f_{7/2})^{-1}$ octet.

The isobaric analog states at 4.82 and 8.58 MeV are observed to be populated in the ($^3$He, $p$) reaction with pure $L_{np} = 0$ transfer. Many other levels above 1.3 MeV and below 4.0 MeV are also observed to be populated by the ($^3$He, $p$) reaction, and the angular distributions of some could be interpreted as $L_{np} = 0 + 2$ mixtures. A mixture of $L_{np} = 0$ and 2 necessitates a $J^\pi = 1^+$ state. Such an angular distribution is observed for the $J^\pi = 1^+$ levels at 1.333 and 1.490 MeV.

Two nuclear models are evaluated by comparing their predictions with the experimental data. The truncated $1f_{7/2}$ spherical shell model of MBZ[1] predicts energy levels and wave functions for $^{50}$V. These wave functions are used to calculate the spectroscopic factors for the levels populated by $l = 3$ transfer in the ($^3$He, $d$) and ($^3$He, $\alpha$) reactions. The energy levels below 1 MeV are seen to be

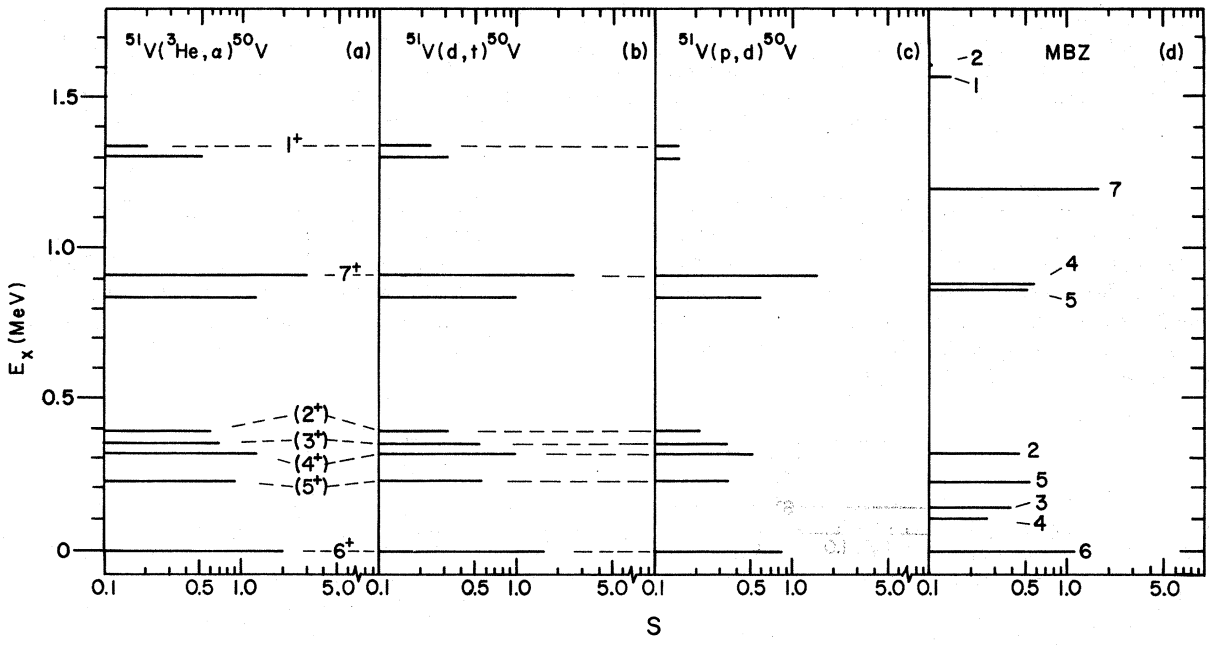


FIG. 15. Spectroscopic factors for neutron pickup reactions to states in $^{50}$V. The measured values for the indicated levels were obtained by DWBA analysis of (a) the $^{51}$V($^3$He, $\alpha$) data (present work), (b) the $^{51}$V($d$,$t$) data (Ref. 6), and (c) the $^{51}$V($p$,$d$) data (Ref. 26). The theoretical predictions (d) were obtained with the MBZ theory.

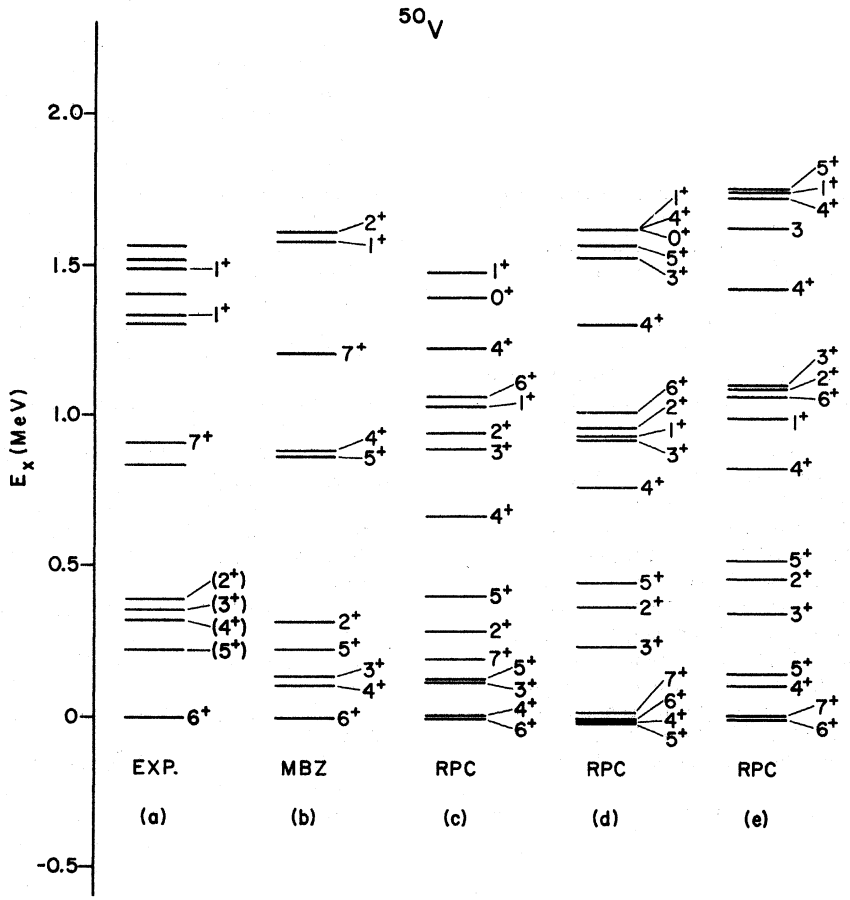


FIG. 16. Energy levels in $^{50}$V. (a) Experimental levels up to 1.6 MeV (b) MBZ predicted levels up to 2.0 MeV. The last three level schemes were calculated with the rotational-particle coupling model with the parameters (Refs. 2 and 10) $A = 0.2$ MeV, $C = -0.28\hbar\omega_0$, $D = -0.06\hbar\omega_0$, and $\hbar\omega_0 = (41 \text{ MeV})/A^{-1/3}$. They differ in that (c) was obtained with $Q = 0.9$, $\beta = -0.25$, and the Kuo-Brown matrix elements, (d) was obtained with $Q = 0.9$, $\beta = -0.3$, and the Yukawa-Rosenfeld matrix elements (Ref. 2), and (e) was obtained with $Q = 0.95$, $\beta = -0.3$, and the Yukawa-Rosenfeld matrix elements.

well reproduced, although the calculations predict an extra $4^+$ and an extra $5^+$ level. The predicted spectroscopic factors are of the right magnitude for the lowest states, even though the ($^3$He, $d$) results show that an admixture of the $2p$ orbital is present in some of the levels, and this orbital is not included in the MBZ calculations.

The other model evaluated is the Coriolis-coupling model with two particles outside a deformed core.[2] This model has been able to reproduce the experimental energy levels about as well as the MBZ calculations, the similarity extending even to predicting an "extra" $4^+$ and $5^+$ level.

---

*Work performed under the auspices of the U. S. Atomic Energy Commission.

†AUA-ANL Indiana University predoctoral fellow; currently at the Ohio State University, Columbus, Ohio 43210.

[1]J. D. McCullen, B. F. Bayman, and L. Zamick, Phys. Rev. 134, B515 (1964); Princeton Technical Report No. NYO-9891, 1964 (unpublished).

[2]P. Wasielewski, Ph.D. thesis, Yale University, 1970 (unpublished).

[3]J. N. Bishop, D. J. Pullen, and B. Rosner, Phys. Rev. C 2, 550 (1970).

[4]P. Blasi, P. R. Maurenzig, N. Taccetti, and R. A. Ricci, Phys. Letters 28, B555 (1969).

[5]G. Bruge, A. Bussiere, H. Faraggi, P. Kossanyi-Demay, J. M. Loiseaux, P. Roussel, and L. Valentin, Nucl. Phys. A129, 417 (1969).

[6]A. Sourkes, H. Ohnuma, and N. M. Hintz, University of Minnesota Tandem Laboratory Annual Report, 1969 (unpublished).

[7]W. F. Buhl, D. Kovar, J. R. Comfort, O. Hansen, and D. J. Pullen, Nucl. Phys. A131, 99 (1969).
[8]S. Hinds, J. H. Bjerregaard, O. Hansen, and O. Nathan, Phys. Letters 21, 328 (1966).
[9]S. Hinds and R. Middleton, Nucl. Phys. A42, 422 (1967).
[10]J. W.Smith, Ph.D. thesis, Indiana University, 1971 (unpublished).
[11]J. R. Erskine, Argonne Split-Pole Magnetic Spectrograph Manual, Argonne National Laboratory, 1969 (unpublished).
[12]J. R. Erskine and R. H. Vonderohe, Nucl. Instr. Methods 81, 221 (1970).
[13]P. Spink and J. R. Erskine, Argonne National Laboratory Physics Division Informal Report No. PHY-1965B (unpublished).
[14]P. D. Kunz, private communication.
[15]D. Bechner, R. Santo, H. H. Duhm, R. Back, and S. Hinds, Nucl. Phys. A106, 577 (1968).
[16]Recently published work on the $^{51}$V($d$,$t$)$^{50}$V reaction [R. DelVecchio, W. Daehnick, D. L. Dittmer, and Y. S. Park, Phys. Rev. C 3, 1989 (1971)] shows the level at 1.330 MeV to be populated by pure $l$ = 3 transfer, in agreement with our results but contrary to the $l$ = 1 + 3 reported by Sourkes, Ohnuma, and Hintz. DelVecchio *et al.* also see $l$ = 3 strength above 1.5 MeV excitation, in agreement with the present ($^3$He,$\alpha$) results; and on the basis of the yield of the $^{52}$Cr($d$,$\alpha$)$^{50}$V reaction, they support the tentative spin assignments of the first four excited states.
[17]J. B. French and M. H. Macfarlane, Nucl. Phys. 26, 168 (1961).
[18]D. J. Pullen, Bull. Am. Phys. Soc. 16, 551 (1971).
[19]R. R. Betts, H. T. Fortune, J. D. Garrett, R. Middleton, D. J. Pullen, and O. Hansen, Phys. Rev. Letters 26, 1121 (1971).
[20]F. C. Ernê, W. A. M. Veltman, and J. A. J. M. Wintermans, Nucl. Phys. 88, 1 (1966).
[21]S. Maripuu, Nucl. Phys. A123, 357 (1969).
[22]Chih Shin, Ph.D. thesis, University of Heidelberg, 1969 (unpublished).
[23]T. H. Braid, L. Meyer-Schützmeister, and D. D. Borlin, in *Isobaric Spin in Nuclear Physics*, edited by J. D. Fox and D. Robson (Academic, New York, 1966), p. 605.
[24]M. Moinester, J. P. Schiffer, and W. P. Alford, Phys. Rev. 179, 964 (1969).
[25]M. N. Rao, J. Rapaport, T. A. Belote, and W. E. Dorenbusch, Nucl. Phys. A151, 351 (1970).
[26]C. A. Whitten, Jr., Ph.D. thesis, Princeton University, 1966 (unpublished).
[27]F. B. Malik and W. Scholz, Phys. Rev. 150, 919 (1966).
[28]W. Scholz and F. B. Malik, Phys. Rev. 147, 836 (1966).
[29]P. Wasielewski and F. B. Malik, Nucl. Phys. A160, 113 (1971).
[30]J. R Comfort, P. Wasielewski, F. B. Malik, and W. Scholz, Nucl. Phys. A160, 385 (1971).
[31]I. Lindgren, in *Alpha-, Beta-, and Gamma-Ray Spectroscopy*, edited by K. Siegbahn (North-Holland, Amsterdam, 1964), Appendix 4.